

## Structural analysis of divalent cation block generated in the prokaryotic sodium channel

Divalent cation blocking was observed in important tetrameric cation channels. For example, magnesium ions block NMDA receptor currents in a voltage-dependent manner [1]. The pore domain of the tetrameric cation channels consists of two transmembrane helices, and a selectivity filter (SF) is located in the loop between them. The SF of the tetrameric cation channels is responsible for the selective permeation of cations. Functional analyses and simulations of NMDA receptors suggested that residues in the SF are involved in magnesium inhibition. However, the detailed molecular mechanism of divalent cation blocking of SFs is not yet fully understood. Prokaryotic Nav (BacNav) provide structural insights into tetrameric channels. NavAb is the most critical contributor of BacNav to the first full-length structure of Nav at atomic resolution [2]. NavAb current is not blocked by divalent cations. Therefore, reproducing the blocking on NavAb and its structural analysis would help elucidate the molecular mechanisms of divalent cation blocking. By introducing mutations into NavAb SF Leu176, we successfully reproduced the divalent cation-blocking effect of the NavAb (Fig. 1) [3].

Interestingly, the divalent cation-blocking mutations can be classified into two types. One is a mutation in a hydrophilic side chain residue, and the other is a mutation in a residue with a small side chain. In contrast, no inhibitory effect was observed for mutations in large side-chain residues in the side

chain. We conducted a crystallographic structural analysis of these mutants using SPing-8 **BL32XU**, **BL41XU**, and **BL45XU** beamlines [3].

We determined the crystal structures of L176Q, L176G mutants, and wild-type channels with and without calcium ions at resolutions of approximately 3 Å (Fig. 2(a)). NavAb has three ion interaction sites in the SF: a high-energy-field site (SiteHFS), a center site (SiteCEN), and an inner site (SiteIN) (Fig. 2(b)). To evaluate electron density, we compared the difference maps between the structures of each mutant with and without calcium ions. In the ionic pathway of the wild-type channel, there was no difference in the density of the calcium ion condition subtracted from the electron density of the no calcium ion condition (Fig. 2(b)). In the L176Q mutant, significant increases in differential density were observed between SiteCEN and SiteIN and below SiteIN (Fig. 2(c)). These increased densities were due to calcium ions, which caused current inhibition. The carbonyl group of the L176Q side chain faces the center of the ion pathway. By comparing the electron densities of the L176Q and wild-type channels under the same ionic conditions, we found that the L176Q side chain was responsible for the increase in electron density below SiteIN (Fig. 2(c)). This suggests that the L176Q mutation can stabilize ions or water at this site more effectively than the wild-type channel can. Therefore, calcium ions were stacked at the center of the ion permeation pathway and blocked the current in the L176Q mutant. In the case of the

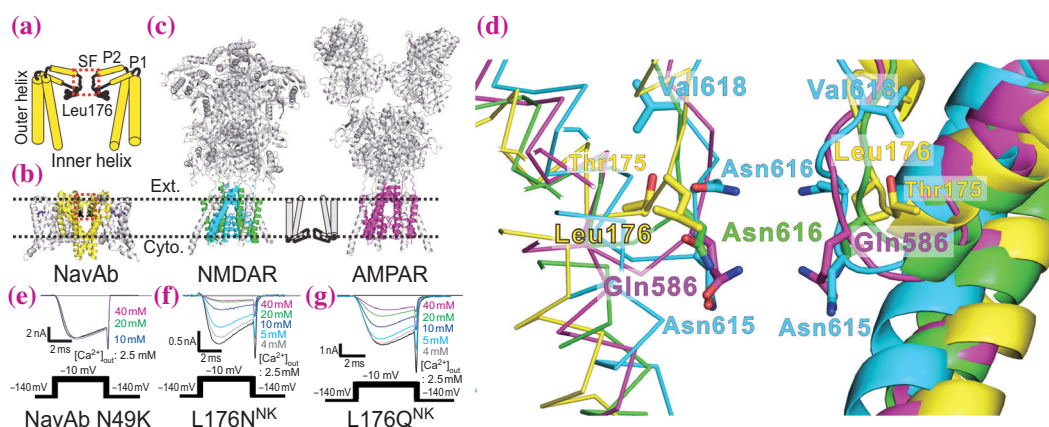


**Fig. 1.** (a, b) Schematic diagram and overall structure of NavAb channel (pdb code; 5yuc). The pore domain is colored yellow. The red dashed square indicates the SF. Leu176 is colored black. (c) Overall structures of NMDAR and AMPAR. The pore domain of NMDAR (pdb code; 4t1m) is colored green (NR1) and cyan (NR2B), and the pore domain of AMPAR (pdb code; 5wek) is colored magenta. (d) The pore domain of NavAb superimposed on that of NMDAR NR1 and NR2b subunit and AMPAR A2 subunit, respectively. (e-g) Representative current traces of NavAb N49K, N49K/L176N, and N49K/L176Q mutants.

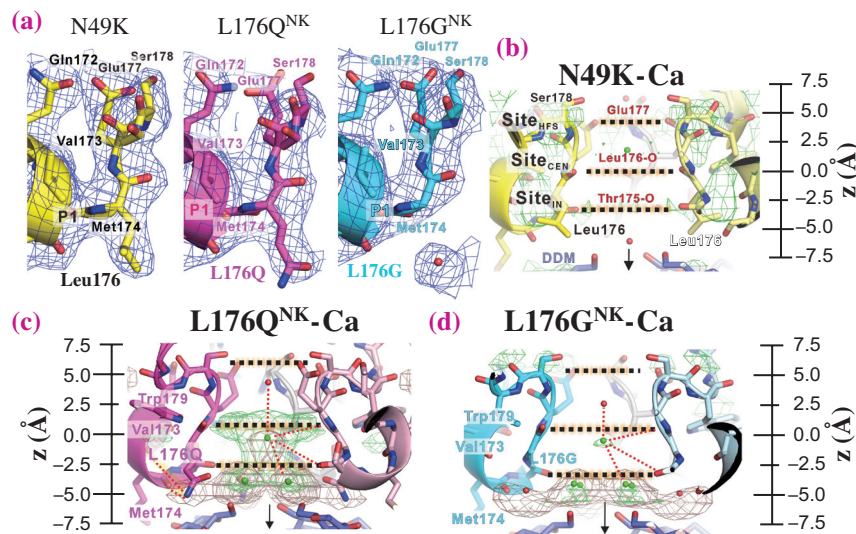


**Fig. 2.** (a) The electron density around residue 176 of the SF. The cartoon view and carbon atoms of NavAb wild-type channel, L176Q, and L176G mutants are colored yellow, magenta, and cyan, respectively. The blue mesh indicates the  $2F_o - F_c$  electron density map contoured at  $1\sigma$ . (b-d) Horizontal view of the SF of NavAb wild-type channel (b), L176Q (c), and L176G (d) mutants. Green mesh indicates the difference-electron density map contoured at  $5\sigma$  of each mutant  $F_o$  in the calcium condition subtracted with that in the non-calcium condition. Brown mesh indicates the differential electron density map contoured at  $5\sigma$  of each mutant  $F_o$  subtracted with wild-type channel  $F_o$ . The upside is the extracellular side.

L176G mutant, the differential density increased because the glycine mutation created an extra cavity at the interface between the SF and inner vestibule (Fig. 2(d)). The electron density of SiteIN in the L176G mutant was also more substantial than that of the wild-type NavAb under calcium ion conditions (Fig. 2(d)). This suggests that calcium ions are stacked around SiteIN and block the current in the L176G mutant.

The crystal structures of these mutants showed an increase in electron density derived from calcium ions at the bottom of the SF. Hydrophilic side chain mutations provide hydrogen bonds to molecules around SiteIN of the SF, allowing calcium ions to stack at SiteCEN (Fig. 3, middle). The small side-

chain mutation of Leu176 creates extra cavities in which the original leucine side chains are located. Including additional water molecules allows divalent cations to interact with water molecules and block the entrance to the inner vestibule (Fig. 3, right), similar to hydrophilic mutations. We proceeded with a molecular dynamics (MD) simulation to analyze the detailed interaction between calcium ions and the mutated side chains of the L176Q and L176G mutants, and our hypothesis was confirmed. BacNavs are the most advanced channel groups, with well-organized structural analyses and simulations. Therefore, our results and methods of structural analysis and MD simulations are expected to play a meaningful role in the advanced analysis of the molecular mechanisms of tetrameric ion channels.

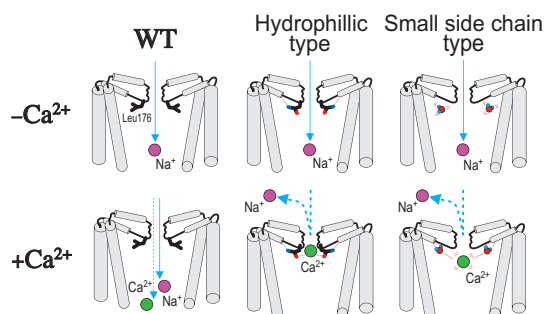


**Fig. 3.** The proposed molecular models of NavAb wild-type, L176Q, and L176G, respectively. Gray cylinders indicate the helices of the NavAb pore domain helices. Green and purple spheres indicate calcium and sodium ions, respectively.

Katsumasa Irie

Department of Biophysical Chemistry,  
Wakayama Medical University

Email: kirie@wakayama-med.ac.jp

**References**

[1] M. L. Mayer *et al.*: Nature **309** (1984) 261.  
 [2] J. Payandeh *et al.*: Nature **475** (2011) 353.  
 [3] K. Irie, Y. Oda, T. Sumikama, A. Oshima, Y. Fujiyoshi: *Nat. Commun.* **14** (2023) 4236.